



Behavior and surface properties of microalgae indicate environmental changes

N. Ivošević DeNardis¹ · N. Novosel Vlašić¹ · T. Mišić Radić¹ · J. Zemla² · M. Lekka² · I. Demir-Yilmaz^{3,4} · C. Formosa-Dague³ · M. Levak Zorinc¹ · I. Vrana¹ · K. Juračić¹ · L. Horvat¹ · P. Žutinić⁵ · M. Gligora Udovič⁵ · B. Gašparović¹

Received: 21 June 2023 / Revised: 14 September 2023 / Accepted: 16 September 2023 / Published online: 13 November 2023
© The Author(s) 2023

Abstract

We conducted a microcosm experiment under near-natural conditions to investigate the effects of environmental stressors temperature and salinity on the response of three microalgal species. The response of microalgae to increased temperature and altered salinity is species-specific, with cell barrier complexity playing an important protective role. At decreasing salinity, the green flagellate cells of *Dunaliella tertiolecta* vibrate around the point and become stiff while their physiological activity is at its highest, which may indicate that organic matter is being released into the medium. At the highest salinity, *Tetraselmis suecica* showed the highest growth rate along with the hydrophobic behavior of the cells, which is a favorable condition for the formation of aggregates. Under these conditions, the cells could enter the cyst stage, while the content of polar lipids could mediate cell adhesion to the natural interfaces. *Cylindrotheca closterium*, a diatom with an organosilicate cell wall, also showed the highest physiological activity at decreasing salinity. However, the cells were softest and exhibited hydrophilic behavior, implying that released organic material could alter the surface properties of the diatom. This study provides insight into the behavioral, mechanical, and molecular changes of microalgae under near-natural conditions, which may contribute to a fundamental understanding of how biochemistry and mechanics interact to control the functional behavior of microalgal cells in climatically altered aquatic systems.

Keywords Cell surface properties · Environmental stress · Hydrophobicity · Microalgae · Motility · Released organic matter

Introduction

Understanding the effects of various environmental stressors on microalgae is critical for assessing the health and function of aquatic habitats, in terms of nutrient cycling and ecosystem stability (Zhang et al. 2022; Kholssi et al. 2023).

Multiple stressors such as temperature, salinity, pH, light intensity, nutrient availability, and pollution can significantly affect the growth, productivity, physiology, and overall status of microalgae by acting independently or interacting with each other, leading to complex cellular responses (Cronin and Hay 1996; Carter et al. 2005; Borowitzka 2018; Schriber and Venable 2019; Wu et al. 2021; Haris et al. 2022; Domingues et al. 2023; Farkas et al. 2023). The response of microalgae to various stressors depends on the species, type, duration and intensity of the stressors. Some microalgae may exhibit tolerance or acclimation mechanisms that allow them to withstand certain stress combinations better than others. However, in many cases, prolonged exposure to multiple stressors can lead to significant declines in microalgal populations, disruption of aquatic ecosystems, and possible cascading effects at higher trophic levels (Häder and Gao 2015; Murphy et al. 2020; Van de Waal and Litchman 2020; Glibert et al. 2022). Stressors can impair photosynthesis,

✉ N. Ivošević DeNardis
ivosevic@irb.hr

¹ Ruđer Bošković Institute, Zagreb, Croatia

² Institute of Nuclear Physics Polish Academy of Sciences, Kraków, Poland

³ Toulouse Biotechnology Institute, Université de Toulouse, INSA, INRAE, CNRS, Toulouse, France

⁴ LAAS, Université de Toulouse, CNRS, Toulouse, France

⁵ Department of Biology, Faculty of Science, University of Zagreb, Zagreb, Croatia

disrupt cellular processes, and even lead to cell death. Various stress conditions, e.g., increased temperature combined with nutrient deficiency, can cause a range of cellular physiological, mechanical, and metabolic changes that promote lipid production, which is essential for biofuel production and other applications (Arbona et al. 2013; Kwak et al. 2016; Flanjak et al. 2022). For example, Bautista-Chamizo et al. (2018) reported increased production of microalgal lipids and carotenoids in *Phaeodactylum tricornutum* cells under synergistic effects of pH, salinity, and temperature.

Deciphering the complex interplay of abiotic stressors on microalgae in aquatic systems can facilitate understanding of how biochemistry and mechanics interact to control the functional behavior of cells. A few laboratory studies have reported results at the single-cell level, focusing specifically on changes in cell surface properties and cell behavior (Pletikapić et al. 2012; Ivošević DeNardis et al. 2019; Pillet et al. 2019; Novosel et al. 2020, 2022a, b; Mišić Radić et al. 2021, 2022; Demir-Yilmaz et al. 2023a, b). The results showed that the response of microalgae was species- and stressor-specific. When the temperature or salinity was reduced, the cells became stiffer, which was accompanied by a change in hydrophobicity that may affect cell aggregation. Due to the strong cellular response, the naked green alga *Dunaliella tertiolecta* showed the greatest chemical and nanomechanical changes. *Tetraselmis suecica*, a green alga with calcite-coated theca, appeared to be temperature-tolerant but salinity-sensitive. In contrast, the diatom *Cylindrotheca closterium* was less vulnerable due to the protective function of its organosilicate cell wall.

In the context of climate change associated with an increase in ocean temperature and a possible decrease in sea surface salinity, this study aims to investigate the response of microalgal species to specific environmental conditions (increase in temperature and decrease in salinity) in a microcosm experiment. Three microalgal species (*D. tertiolecta*, *T. suecica*, and *C. closterium*) were selected as model organisms because they differ in cell barrier complexity and are common in marine systems. The selected salinity ranges represent shifts in the salinity spectrum of marine systems from the euhaline to the mesohaline range. We combined bulk analytical methods to characterize cell cultures in terms

of growth dynamics, motility, physiological activity, and lipid profiling and surface methods to characterize single cells and the release of extracellular material in terms of surface properties and structural organization, respectively. The combination of methods used will provide additional information linking the molecular and nanometer scales. The results will allow us to better understand the mechanisms of algal cell acclimation and the potential protective function of the cell barrier under perturbed, near-natural conditions.

Materials and methods

Microcosm setup

Three different species of marine algae were selected: *Dunaliella tertiolecta* (DT, Chlorophyta, CCMP 1320, Culture Collection Bigelow Laboratory for Ocean Sciences, Bigelow, MN, USA), *Tetraselmis suecica* (TS, Chlorophyta, CCAP 66/22A, Culture Collection of Algae and Protozoa, Scottish Marine Institute, Oban UK), and *Cylindrotheca closterium* (CC, Bacillariophyta, CCMP 1554, Culture Collection Bigelow Laboratory for Ocean Sciences). Microalgal cells were cultured in 1 L of F/2 medium (Guillard 1975) prepared with natural seawater filtered through Whatman filters with a pore size of 0.22 µm and three selected salinities: 19, 27 and 38. Cell cultures were grown outdoors in a natural light–dark cycle in 2 L Nalgene PC bottles. A total of 18 bottles of cell cultures (2 replicates of one cell culture per salinity) and 6 bottles of seawater (2 replicates of the corresponding salinities as controls) were placed in a swimming pool in a location with maximum possible daily sunlight from September 8 to 14, 2022 (Fig. 1). Stable and sunny weather conditions prevailed for 7 days. The sun rose at 6:25 a.m. and set at 7:21 p.m., so the duration of sunlight was 12 h and 57 min.

The swimming pool had the following characteristics: volume 960 L, height 70 cm, outer diameter 2.04 m, inner diameter 1.60 m. To ensure good mixing of the samples, a nozzle was placed at the bottom of the pool operated by a water pump in a closed circuit. This nozzle was placed at the edge of the basin at an angle of about 45°, creating waves

Fig. 1 Microcosm experimental setup in an outdoor swimming pool at the Ruđer Bošković Institute, Zagreb, Croatia



and counterclockwise circulation of the water in the basin. The bottles containing the 1 L samples were allowed to float freely at 2 rpm within the perimeter of the basin, with an observed wave amplitude of 1–5 cm. A digital temperature logger was placed in the pool to record the water temperature every 10 min (Fig. 2).

The fluctuations in air temperature followed the same pattern as the fluctuations in pool water temperature. The water temperature was on average 3 °C higher than the air temperature. Cell cultures were grown at water temperature of 28–33 °C. To ensure cultivation of selected microalgal species under selected environmental stressors, a series of replicate experiments (at salinities of 19, 27, 38 and a temperature of 30 °C) were performed in a water bath under controlled laboratory conditions (constant shaking (20 rpm), 12 h:12 h light:dark cycle with an irradiance of 31 $\mu\text{mol photons m}^{-2} \text{s}^{-1}$). Cell numbers in replicate samples were determined each day using a Fuchs-Rosenthal hemocytometer (Fein-Optik Jena, Germany, depth 0.2 mm) and a light microscope (Olympus BX51, Olympus Corporation, Japan). The growth rate and doubling time of cells were determined in the exponential growth phase from day 3 to day 5 (Kim 2015). In the stationary growth phase (day 7), cells were centrifuged ($2000 \times g$, 3 min) and pellets were resuspended twice with seawater. The stock cell suspension was prepared by resuspending the last pellet in 2 mL of filtered seawater with the appropriate salinity.

Confocal microscopy

Confocal measurements were carried out using an oil immersion objective ($63 \times$ magnification) and a white-light laser on a Leica TCS SP8 Laser Scanning Confocal Microscope (Leica Microsystems GmbH, Germany). The spectral scan option was used to improve the emission and excitation wavelengths ranges. Autofluorescence of algal cells was

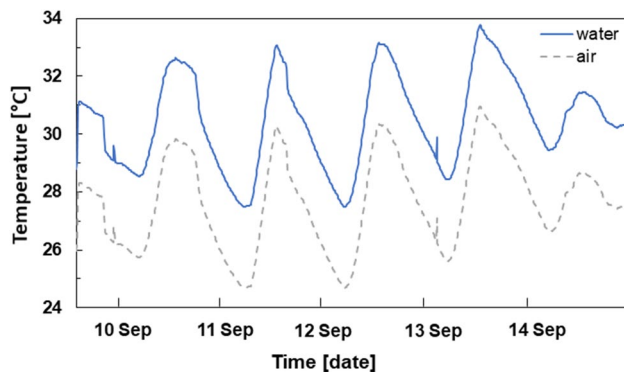


Fig. 2 Variation of water and air temperatures in the swimming pool during the microcosm experiment conducted in September 2022

detected at a maximum excitation wavelength of 650 nm and a detection wavelength range of 720–750 nm.

Sample preparation for confocal imaging

Slides for confocal microscopy were washed in glass beakers with ethanol followed by ultrapure water. The slides were dried with a stream of nitrogen. An aliquot of 50 μL of 0.2% (w/v) polyethyleneimine (PEI, Sigma Aldrich Corporation, USA) was added to the center of the clean slide to prepare for cell immobilization and allowed to settle for 30 min. After removing the PEI droplet, the center of the slide was rinsed three times with ultrapure water. Then, 20 μL of the cell cultures were added to the center of the slide and allowed to settle. The slides were kept in a Petri dish with moist absorbent paper until imaging to prevent evaporation of the droplets. Prior to imaging, samples were stained with DAPI (Sigma), Alcian blue (Sigma), and Dil (Sigma) by diluting 20 \times stock solutions.

Motility analysis

The motility of cells was recorded as 10 consecutive video clips (.avi format, duration 5 s, 50–60 frames per second, image size: 340×250 , 4×4 binning) under an Olympus BX51 microscope ($10 \times$ magnification). For analysis of cell motility and trajectories, video data were fed into the open-source image processing software ICY (<http://icy.bioimageanalysis.org>; Novosel et al. 2020). The Spot Tracking, Track Manager, and Motion Profiler plug-ins were used. ICY produced an ASCII file that contained the sample size, spatiotemporal position of the cells, number of motile and non-motile cells, minimum, median, arithmetic mean, and maximum speeds and search radius. The search radius is defined as the farthest distance a cell can travel from its origin. Data from around 300 cell analyses were imported into Microsoft Excel (Microsoft Corporation, USA). The software tool RStudio was used for additional statistical analyses (R Core Team 2022; RStudio Team 2023). Boxplots of cell speed and search radius were generated. The Shapiro–Wilk normality test (Royston 1995) and the pairwise Wilcoxon rank sum tests (Bauer 1972; Hollander and Wolfe 1999) implemented in R were used to examine the distributions and compare the mean values of cell speed and search radius under environmental stressors in near-natural conditions.

Electrochemical method

Molecular adsorption on the dropping mercury electrode (DME) was used to characterize the organic constituents, such as biopolymers and sub-micrometer particles, in the aqueous electrolyte solution using the electrochemical method of polarography (Žutić et al. 1999, 2004; Svetličić

et al. 2006; Pletikapić and Ivošević DeNardis 2017). Adsorption of organic molecules on DME is recorded as a gradual decrease in the reduction current, which is proportional to the surfactant concentration in the sample and is referred to as surfactant activity. Surfactant activity provides an alternative method for determining the amount of dissolved organic carbon in seawater (Hunter and Liss 1981). The polarographic maximum of Hg(II) ions can be used to evaluate surfactant activity, expressed in milligrams per liter as the equivalent amount of the non-ionic synthetic surfactant Triton-X-100 (polyethylene glycol tert-octylphenyl ether).

Electrochemical measurement of cell sample

Cell samples were characterized electrochemically using a three-electrode system in an air-permeable and thermostatic Metrohm vessel. The working electrode, DME, had the following characteristics: drop time of 2.0 s, flow rate of 6.0 mg s^{-1} , and maximum surface area of 4.57 mm^2 . All potentials were compared to a potential measured on a reference electrode. This consisted of a ceramic frit separated from the measured dispersion by Ag/AgCl (0.1 M NaCl). The counter electrode consisted of a platinum wire. An aliquot of the cell suspensions was mixed with 25 mL of filtered seawater (pH 8.0) and placed in a Metrohm vessel at 20°C . A 174A Polarographic Analyzer (Princeton Applied Research, USA) was connected to a computer for electrochemical measurements. Analogue data were acquired using a DAQ card-AI-16-XE-50 (National Instruments, USA). The program written in LabView 6.1 software (National Instruments) was used to analyze the data. Cell samples were electrochemically characterized by recording polarograms of oxygen reduction (current–potential curves). Prior to the measurement of surfactant activity, 0.5 mL of 0.1 M HgCl_2 was added to the sample.

Atomic Force Microscopy (AFM)

A Multimode Scanning Probe Microscope with a Nanoscope IIIa controller (Bruker, USA) and a vertical engagement (JV) 125 m scanner were used to image cells and released extracellular polymers. A DNP probe (Bruker) with a nominal spring constant of 0.06 N m^{-1} and a nominal frequency of 18 kHz was employed for contact mode imaging in air. The scan resolution was 512 samples per line and the linear scan rate was optimized between 1.5 and 2 Hz. To reduce the forces between the tip and the surface, the set point was kept as low as possible. Image analysis was performed using NanoScope™ software (NanoScope Analysis, version 2.0; BrukerUSA).

Sample preparation for AFM imaging of cells and released extracellular polymers

Samples for AFM imaging of cells and released extracellular polymers were prepared according to a previously established protocol (Novosel et al. 2022a, b). Briefly, cells of DT, TS, and CC were separated from the growth medium by centrifugation (Section 2.1). The collected pellets were then used to prepare samples for AFM. Unmodified mica was used as the substrate for the DT and CC samples, while PEI-modified mica was used for the TS sample. The sample preparation protocol for AFM imaging only required fixation of the DT suspension. Prior to AFM imaging, samples were rinsed three times with ultrapure water to remove excess salt crystals and dried in closed Petri dishes for 45 min.

Atomic force microscopy working in force spectroscopy mode

Mechanical properties of algal cells were measured using AFM JPK NanoWizard 4 XP (Bruker) operating in force spectroscopy mode. The microscope is integrated with an inverted optical microscope (Olympus IX73, Olympus Corporation, Japan) using LUCPLFLN40XP objective (Olympus Corporation), which allows direct superposition of the optical image of the sample and the scan area. A silicon nitride pyramid probe, MLCT-D (Bruker) with a nominal spring constant of 0.03 N m^{-1} , a nominal frequency of 15 kHz, and the half-open angle of the probe of 21° was used. The cantilever spring constants were calibrated using the thermal noise method (Sader et al. 1995). Force curves were recorded over a $3 \mu\text{m} \times 3 \mu\text{m}$ area in the central part of the cell at an approach and retraction velocity of $8 \mu\text{m s}^{-1}$ and a loading force of 2 nN. A grid of 4×4 force curves was recorded. The number of cells measured varied from 20 to 35 cells.

The mechanical properties of the CC cells were measured using the Nanowizard III AFM system (Bruker). Force spectroscopy experiments were performed with a force between 1 and 2 nN using MLCT AUWH cantilevers with nominal spring constants of 0.01 N m^{-1} . Nanoindentation measurements were performed on 7 cells, and 400 force curves were recorded on areas of $1 \mu\text{m} \times 1 \mu\text{m}$ on the cell surface.

Measurements for all three species were performed at salinities of 19, 27, and 38. JPK data processing software (Bruker-JPK, Germany), version 7.0.165 was used for data analysis.

Elasticity determination

The apparent Young's modulus (elasticity parameter, E) for DT and TS was determined by applying the Hertz-Sneddon contact model (Hertz 1881; Sneddon 1965), which relates

the loading force (F) and the indentation depth (δ) in the case of a four-sided pyramid probe as follows:

$$F = \frac{E}{1 - \nu^2} \frac{\tan \alpha}{\sqrt{2}} \delta^2 \quad (1)$$

In the equation above, α is a half-open angle of the indenting probe and ν is Poisson's ratio equal to 0.5 because we assume incompressibility of the algal cells. The maximum indentation depth did not exceed 2 μm and the model was fitted to the AFM data over the entire range of indentation depth. The value E of CC was calculated from 50 nm indentation curves using the Hertz-Sneddon model (Hertz 1881; Sneddon 1965) for a conical indenter in which the force F , indentation depth (δ), and E follow Eq. (2):

$$F = \frac{2E \tan \alpha}{\pi(1 - \nu^2)} \delta^2 \quad (2)$$

Here α is the opening angle of the tip (17.5°) and ν is the Poisson's ratio (arbitrarily assumed to be 0.5). The spring constants of the cantilevers were determined before each experiment using the thermal noise method (Hutter and Bechhoefer 1993).

The calculated E is given as median and first (Q1) and third (Q3) quartiles. Statistical comparisons of the results obtained in each case were performed using an unpaired t-test, which allowed us to compare the means of two independent groups ($p < 0.001$).

Hydrophobic properties of cells

The hydrophobic properties of DT and TS were quantified by comparing AFM data obtained with unmodified and trichlorooctadecylsilane (OTS; Sigma-Aldrich) functionalized MLCT-D probes. The vapor deposition of the OTS silane containing hydrophobic $-\text{CH}_3$ functional groups was performed in a vacuum (2 h exposure). The adhesion properties of cells were quantified by the work of adhesion (W_{adh}) parameter, which was determined from the negative part of the retraction force curve. The forces acting between the algal cell and the probe (unmodified and $-\text{CH}_3$ -modified) during the duration of the experiment cause deflection of the cantilever. The functionalization of the probe was performed immediately before the measurements. The probe speed, scan range, map density, and number of cells examined were the same as those used in the mechanical studies (Section 2.9). The degree of algal cell hydrophobicity (ΔW_{adh}) was determined using the following equation:

$$\Delta W_{\text{adh}} = W_{\text{adh}(\text{noOTS})} - W_{\text{adh}(\text{OTS})} \quad (3)$$

where $W_{\text{adh}(\text{noOTS})}$ and $W_{\text{adh}(\text{OTS})}$ are the work of adhesion extracted from force curves collected with bare and CH_3 -functionalised AFM cantilevers, respectively.

In the case of CC, hydrophobic properties were studied using a recently developed method consisting of measuring the interactions between a bubble (hydrophobic surface) and cell surfaces using Fluidic Force Microscopy (FluidFM; Demir et al. 2021). For this purpose, FluidFM probes with an aperture of 8 μm in diameter (Cytosurge AG, Opfikon, Switzerland) were hydrophobized by coating with self-assembled monolayers (SAMs) of silanes using SAMs vapor deposition technique. The FluidFM cantilevers were functionalized with 1H,1H,2H,2H-perfluorodecyltrichlorosilane (FDTS) using an Orbis-1000 equipment (Memsstar, UK) to make their outer and inner microchannel surfaces hydrophobic. The deposition was carried out under vacuum at 40 Torr and -40°C for 5 min. Then, the microchannel of these silanized cantilevers was filled with air and the probe was immersed in PBS 1X. A slight overpressure of 20 mbar was applied to remove any particulate or dust contamination or to prevent clogging of the FluidFM cantilever. A positive pressure of 200 mbar was then applied inside the microfluidic cantilever in buffer to create a bubble at the opening of the cantilever. The silanized probes were calibrated using the thermal noise method before each measurement (Hutter and Bechhoefer 1993). The interactions between the generated bubbles and CC cells were then recorded under different conditions in force spectroscopy mode, applying a maximum force of 1 nN and a constant retraction speed of 2 $\mu\text{m s}^{-1}$. For each condition, areas of 0.5 $\mu\text{m} \times 0.5 \mu\text{m}$ were examined on 5 different cells. Adhesion forces were determined by calculating the maximum adhesion force from the obtained retraction force curves.

Sample preparation for force spectroscopy measurements

PEI-coated microscopic glass slides were used as substrates for immobilization of algal cells. A volume of 200 μL of a 0.1% PEI solution was added to a clean (ethanol and dH_2O sonication for 15 min each) glass slide and dried overnight.

Cell suspensions were prepared according to protocols optimized for each of the cell types studied. In the case of CC, a 200 μL cell suspension was placed on a substrate for 1 h. The sample was then rinsed 3 times with 200 μL of filtered seawater. The following procedure was used to isolate cells from DT and TS cultures. An aliquot of 1.5 mL of the DT and TS cultures was transferred to Eppendorf tubes. The suspensions were then centrifuged at $265 \times g$ for 3 min and at $940 \times g$ for 5 min (DT and TS, respectively). Then, 1 mL of the medium was removed and the pellet was vortexed. An additional volume of seawater (1 mL) was added to the cell suspensions and centrifuged at the same speed and duration. The supernatant was removed and the cells were resuspended in 400 μL of the filtered seawater. Next, 100 μL of cell suspension was added on a PEI-coated glass slide. After 30 min, the samples were

rinsed 3 times with 100 μL of filtered seawater and measured with AFM.

Lipid extraction

For the determination of lipid classes we collected 100–200 mL of cell culture suspension which was filtered through 0.7 μm Whatman GF/F filters and pre-combusted at 450 $^{\circ}\text{C}$ for 5 h. Lipids were extracted according to a slightly modified protocol of Bligh and Dyer (1959): 10 mL dichloromethane/methanol/deionized water (1:2:0.8 v/v/v) was added to the sliced filters in the cuvettes, along with methyl stearate, which was added as an internal standard to calculate lipid recovery. After 3 min of sonication the filters were stored in dichloromethane/methanol/deionised water overnight at 4 $^{\circ}\text{C}$. Afterwards, the mixture of filter and monophasic solution was filtered through a sinter funnel into a separatory funnel, washed with 10 mL of monophasic solution, and washed with 10 mL of dichloromethane/0.73% NaCl (1:1 v/v) solution mixture. The lipids dissolved in dichloromethane were collected and the extraction was performed again with 10 mL of the dichloromethane. The extracts were evaporated to dryness under nitrogen gas and redissolved in 50 μL of dichloromethane before analysis.

Lipid analysis

Lipid classes were analyzed by thin-layer chromatography/flame ionization detection (TLC/FID; Iatroscan MK-VI, Mitsubishi Kagaku Iatron, INC, Japan). Separation of lipid classes was performed using Chromarods SV and quantified by external calibration with a standard lipid mixture. Hydrogen flow was set at 160 mL min^{-1} and air flow at 2000 mL min^{-1} . The standard deviation determined from duplicate runs ranges from 0.00–0.42 pg cell^{-1} and depends on the lipid class and microalgae. This technique detects 18 lipid classes (hydrocarbons, steryl esters (SE), fatty acid methyl esters, ketones, triacylglycerols, free fatty acids, alcohols, 1,3- and 1,2-diacylglycerols, sterols, pigments, monoacylglycerols, three glycolipids (monogalactosyldiacylglycerols, digalactosyldiacylglycerols, sulfoquinovosyldiacylglycerols), three phospholipids (mono- and di-phosphatidylglycerols, phosphatidylethanolamines and phosphatidylcholines). The separation involved subsequent elution in solvent systems of increasing polarity followed by partial combustion of the Chromarods (Gašparović et al. 2015, 2017). For this work we considered cell lipids as nonpolar polar, and also membrane lipids.

Results

Microalgal growth dynamics

We conducted a microcosm experiment involving three microalgal species (DT, TS, CC) grown at three selected salinities and elevated temperature to mimic environmental stressors under near-natural conditions. Figure 3 shows the growth curves of DT, TS and CC at salinities of 19, 27, and 38, respectively, and pool water temperatures of 28 to 33 $^{\circ}\text{C}$. The initial number of inoculated cells in the growth media was approximately 5.0×10^4 cells mL^{-1} for all species studied. On day 7, all cells mostly entered stationary phase and samples were collected for further characterization. Table S1

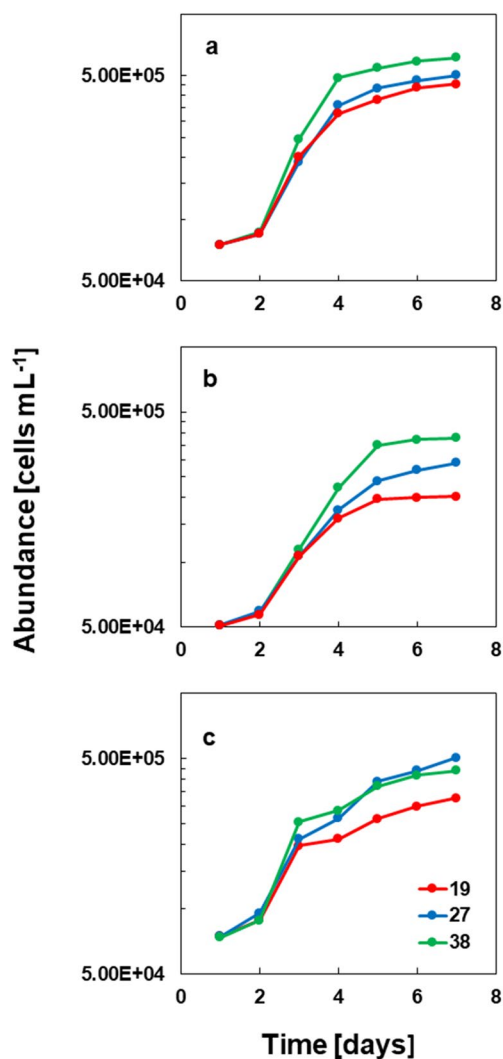


Fig. 3 Growth curves of *Dunaliella tertiolecta* (a), *Tetraselmis suecica* (b), and *Cylindrotheca closterium* (c) under environmental stressors in near-natural conditions. The error in determining cell abundance was up to 10%

summarizes the growth rate and doubling time for each cell species under the selected conditions. The fastest growth and thus the shortest doubling time were obtained for DT and CC at salinity of 27, and for TS at salinity of 38.

Fig. S1 shows representative overlaid confocal images of DT, TS, CC cell cultures under environmental stressors in near-natural conditions. Confocal images of DT cultures at salinities of 38 and 27 showed single microalgal cells with a strong autofluorescence signal, the presence of single bacteria, while at salinity 27 some aggregates were found. In contrast, at salinity of 19, major morphological changes occurred in the DT cells including granular surface structure, detached flagella, some cell aggregates, and the presence of bacteria. In the TS cell culture, cells appeared without flagella at all salinities; at salinity of 19, the autofluorescence signal was weak, cells formed no aggregates, and no bacteria were detected. Confocal imaging of CC cultures at salinities of 38 and 27 showed a few aggregates, very few individual bacteria, and some amorphous particles. At salinity of 19, the cell rostra became curved, and some bacteria and amorphous microaggregates were visible. No bacterial aggregates were observed with DAPI staining.

Motility of flagellated species

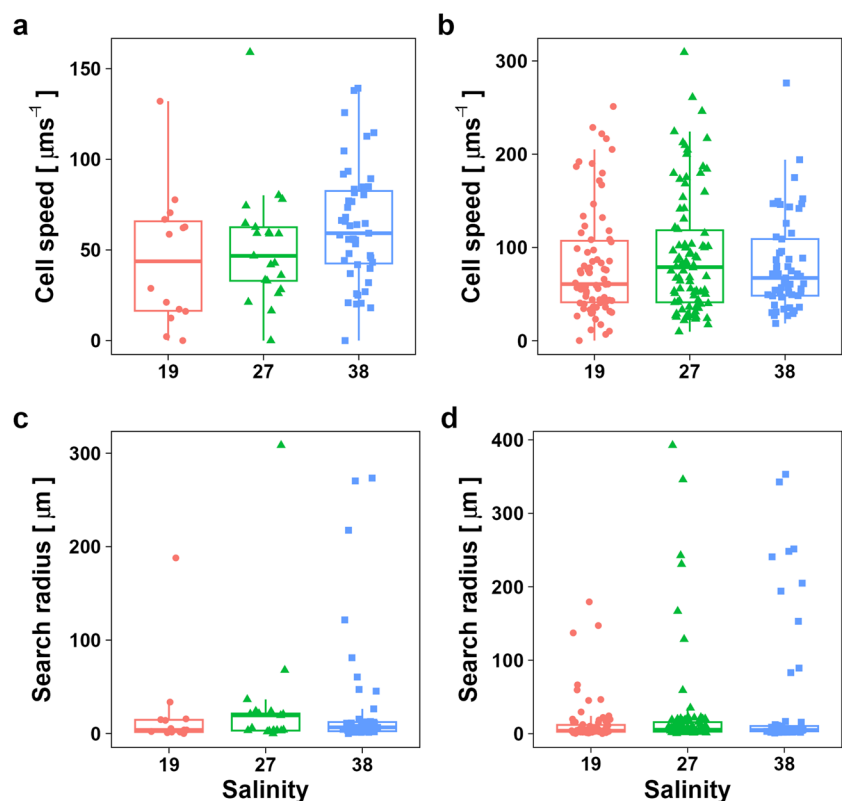
Fig. S2 shows the reconstructed trajectories of individual DT cells under environmental stressors in near-natural

conditions. At salinity of 19, 43% of the cells were nearly immobile or vibrated at the spot. At a salinity of 27, 19% of the cells were static, while the rest moved. At salinity of 38, the majority of cells (72%) showed significant motility. At salinities of 19, 27, and 38, the average speed of vibrating and motile cells were 14, 27, and 30 $\mu\text{m s}^{-1}$ and 68, 57, and 76 $\mu\text{m s}^{-1}$, respectively (Table S2.1).

Figure 4a shows box plots of cell speed for the entire DT population. The median speed at salinities of 19, 27, and 38 were 44, 47, and 59 $\mu\text{m s}^{-1}$, respectively (Table S2.2a). Figure 4c shows box plots of the search radius of DT cells. For salinities of 19, 27, and 38, the median search radii were 4 μm , 19 μm , and 7 μm , respectively (Table S2.2b). At salinities of 19, 27, and 38, the set of cells that moved regularly had an average search radius of 35 μm , 36 μm , and 39 μm , respectively. According to the results of the Shapiro–Wilk normality test, the data for search radius and average speed do not follow the normal distribution (Table S3.3), except for the results at DT for salinities of 19 and 38. There was a weak indication that lower salinity decreased average speed for both DT and TS, but the results of the Kruskal–Wallis ANOVA test showed that this variation in average speed and search radius were not statistically significant (Table S3.4).

Fig. S3 shows the reconstructed trajectories of individual TS cells under environmental stressors in near-natural conditions. At salinity of 19, 33% of the cells were nearly immobile. At salinity of 27, 27% of the cells were static, while

Fig. 4 Box plots for cell speed and search radius for the species *Dunaliella tertiolecta* (a, c) and *Tetraselmis suecica* (b, d) under environmental stressors in near-natural conditions. A whiskered box reflects the median interquartile range (Q3–Q1)



the rest were moving. At salinity of 38, 23% of cells were nearly immobile, while the majority of cells (77%) showed significant motility. At salinities of 19, 27, and 38, the average speed of vibrating and motile cells were 47, 32, and 31 $\mu\text{m s}^{-1}$ and 99, 114, and 93 $\mu\text{m s}^{-1}$, respectively (Table S3.1).

Figure 4b shows the box plots of the cell speeds for the entire TS population. The median cell speeds were 61 $\mu\text{m s}^{-1}$, 79 $\mu\text{m s}^{-1}$, and 67 $\mu\text{m s}^{-1}$ for salinities of 19, 27, and 38 (control), respectively, with no statistically significant deviation from the control (Table S3.2a). The average speed of a set of uniformly moving cells grown at 19, 27, and 38 was 99 $\mu\text{m s}^{-1}$, 114 $\mu\text{m s}^{-1}$, and 93 $\mu\text{m s}^{-1}$, respectively (Table S3.1). Box plots with search radius for the TS cells are shown in Fig. 4d. The median search radius at salinities of 19, 27, and 38 were 4 μm , 5 μm , and 5 μm , respectively. The group of substantially moving cells grown at salinities of 19, 27, and 38 had an average search radius of 22 μm , 33 μm , and 54 μm , respectively (Table S3.2b).

Electrochemical characterization of released surface-active organic matter

The cell releasing surface-active organic matter can be determined by measuring the current–potential curves of Hg(II), which is proportional to surfactant activity. The sample's surfactant activity is a quantitative assessment of the physiological activity of the cells exposed to environmental stressors in near-natural conditions. The results showed that the surfactant activity of the cells increased steadily as the salinity decreased to 19 (Fig. 5). At salinity of 19, all cells studied had the highest surfactant activity, with the TS cell culture having the highest surfactant activity.

Nanoscale imaging of algal cell and released extracellular polymers

The morphology of algal cells exposed to environmental stressors in near-natural conditions was characterized by AFM. All three species maintained the same basic shape regardless of the conditions chosen (Fig. 6a, c, e). The cells of DT had an ovoid shape and contained two flexible flagella. At all salinities studied, the cells of TS had an ellipsoidal shape, and the cell surface had granular features, while all four flagella were absent. The cells of CC had an elongated shape with flexible rostrae that were distinct from the center of the cell. The raphe, valve, and girdle band, three morphologically distinct elements, were all visible on the cell. The morphological parameters of the cells (length, width, height, and surface roughness) that had grown under environmental stressors are shown in Table S4. The length of the cells of DT grown at salinities of 27 and 38 was similar and lower than that of the cells grown at salinity of 19, while the height at salinity of 19 showed the lowest value. The

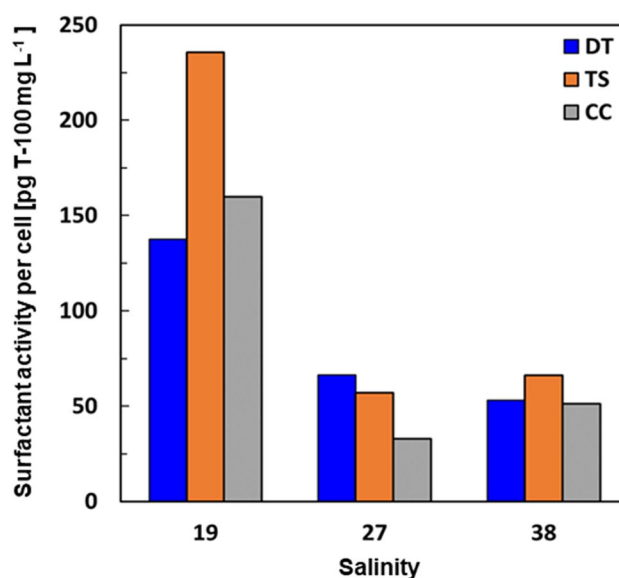


Fig. 5 Surfactant activity of studied algal species (DT: *Dunaliella tertiolecta*, TS: *Tetraselmis suecica*, CC: *Cylindrotheca closterium* under environmental stressors in near-natural conditions

length and height of the cells of TS increased with increasing salinity, while the width of the cells was similar at all three salinities. The length and width of the cells of CC were similar at all salinities, while the height showed the highest value at salinity of 19.

The supramolecular organization of released extracellular polymers (EPS) of DT, TS, and CC cells exposed to environmental stressors was characterized by AFM (Fig. 6b, d, f). We chose the salinity at which the supramolecular organization of extracellular polymers was representative of the species at all salinities (DT and CC), or at which there was a large change in the organization of extracellular polymers (TS). The material surrounding the cells of DT was largely in the form of single and aggregated globules, with just a few fibrils and no fibrillar network found at all salinities. A fibrillar network was observed around the cells of TS grown at salinity of 38, while spherical material, fibrils, and network fragments were observed at salinities of 19 and 27. Around the cells of CC, grown at all salinities, there was mainly spherical material, while some fibrils appeared at salinity of 38.

Nanomechanical characterisation of algal cells by AFM

Algal cells exposed to environmental stressors under near-natural conditions showed a change in mechanical properties (Fig. 7). At salinity of 38, the elasticity parameter E , which quantifies the mechanical properties

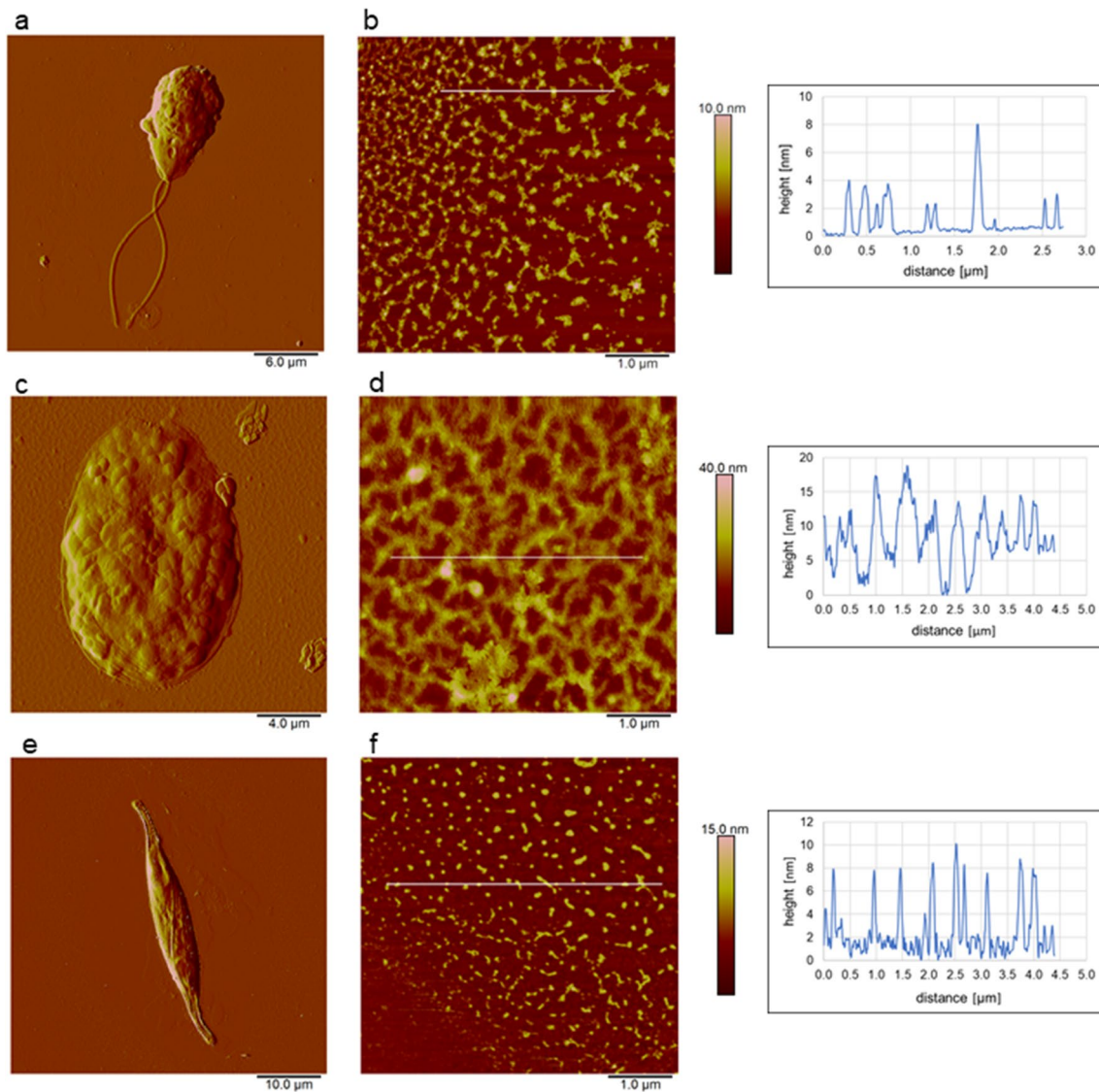


Fig. 6 AFM images of the studied algal cells and EPS under environmental stressors in near-natural conditions. Cell of *Dunaliella tertiolecta* grown at salinity of 19 (a); EPS material around the *D. tertiolecta* cell with vertical profile along the indicated line (b); *Tetraselmis suecica* cell grown at salinity of 38 (c); EPS network around the *T. suecica* cell with vertical profile along the indicated line (d); cell of *Cylindrotheca closterium* grown at salinity of 27 (e); EPS material

around *C. closterium* with vertical profile along the indicated line (f). Images were acquired in contact mode in air and presented as deflection data (a, c, e) and height data with vertical profiles along the indicated lines (b, d, f). Scan sizes: 30 $\mu\text{m} \times 30 \mu\text{m}$ (a); 5 $\mu\text{m} \times 5 \mu\text{m}$, vertical scale 100 nm (b); 20 $\mu\text{m} \times 20 \mu\text{m}$ (c); 5 $\mu\text{m} \times 5 \mu\text{m}$, vertical scale 40 nm (d); 50 $\mu\text{m} \times 50 \mu\text{m}$ (e); 5 $\mu\text{m} \times 5 \mu\text{m}$, vertical scale 15 nm (f)

of DT, was 1.1 kPa as the median value (2.4 kPa as the mean value). As salinity decreased (27 and 19), the cells became stiffer and E increased to 2.4 (3.8) kPa and 3.9 (3.9) kPa, respectively. TS was also stiffer under unfavorable salinity conditions. With increasing salinity, the values of E decreased from 30 (51) kPa and 30 (55) kPa at salinities of 19 and 27, respectively, to 24 (37) kPa at salinity of 38. In contrast, CC was less deformable at salinity of 38 ($E = 819$ (1035) kPa) and the E value decreased 2.5-fold at lower salinity.

Hydrophobic properties of algal cells

The influence of environmental stressors on the hydrophobic properties of DT, TS, and CC under near-natural conditions was determined by AFM force spectroscopy studies. The results showed that regardless of salinity, the outer parts of CC were hydrophilic (Table 1). A similar qualitative trend was observed for DT cells. Only TS showed a transition from a nearly-neutral (unfavorable growth conditions) to a hydrophobic state (salinity of 38).

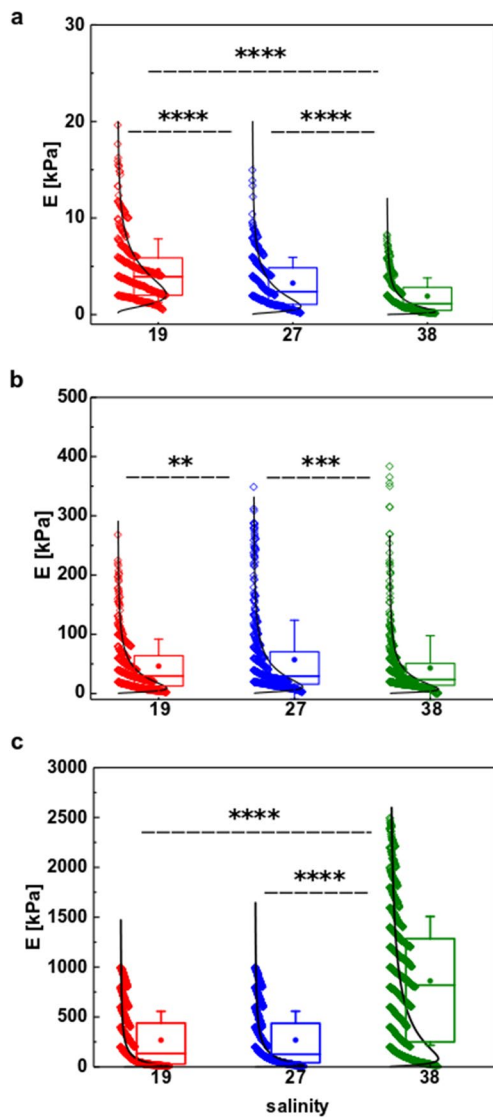


Fig. 7 Box plots depicting Young's modulus distributions for *Dunaliella tertiolecta* (a), *Tetraselmis suecica* (b), and *Cylindrotheca closterium* (c) cells under environmental stressors in near-natural conditions. A whiskered box reflects the median interquartile range (Q3–Q1). The Kruskal–Wallis ANOVA test yielded statistical significance at the level of 0.05 (**** $p < 0.0001$, *** $p < 0.001$, ** $p < 0.01$, * $p < 0.05$)

Table 1 Hydrophobic properties of algal cells under environmental stressors in near-natural conditions. Hydrophilic properties are indicated by (+) and hydrophobic behavior by (-). A value of zero indicates an equilibrium between hydrophobic and hydrophilic components on the cell surface

S	<i>D. tertiolecta</i>	<i>T. suecica</i>	<i>C. closterium</i>
19	+	0	+
27	+	0	+
38	+	-	+

In addition, the degree of hydrophobicity was quantified with ΔW_{adh} (Fig. S4). The highest ΔW_{adh} value for DT (0.409 ± 0.038 fJ) was obtained at the lowest salinity. As salinity increased, the dominance of hydrophilic properties decreased, ΔW_{adh} of 0.222 ± 0.031 fJ. An opposite behavior was observed for TS, which was characterized by strongly hydrophobic properties at salinity of 38 ($\Delta W_{adh} = -0.57 \pm 0.11$ fJ).

Lipid characterization of algal cells

The change in the amount of polar and nonpolar lipids per cell under selected environmental stressors for the three microalgal species studied is shown in Fig. 8. The change in the proportion of polar lipids relative to total cell lipids is also indicated. The content of cell lipids was the highest in TS, but it was salinity-dependent. The lowest content was observed at the more favorable condition of salinity of 38. At salinities of 27 and 19, the cell lipid content increased along with the increase in the relative content of polar lipids compared to salinity of 38. Unlike the other two microalgae, CC had a higher relative content of polar lipids than nonpolar lipids, with the content of polar lipids increasing with decreasing salinity from 38 to 19. The cell lipid content of DT was the lowest among the three microalgae studied. The relative content of polar lipids decreased from a salinity of 38 to a salinity of 19 in both green microalgae studied, DT and TS.

The content of membrane lipids of the studied DT, TS and CC followed that of cell lipids (Fig. 9). The data showed that the content of sterols, glycolipids and phospholipids increased with decreasing salinity in all microalgal species.

Discussion

We studied the response of three microalgal species exposed to environmental stressors under near-natural conditions in a microcosm experiment and compared it to our previously reported laboratory studies with single stressors (Novosel et al. 2022a, b). The microcosm experiment was conducted outdoors where natural light intensity, its duration, and temperature varied throughout the day. The temperature in the pool varied in a range of 28–33 °C, while the laboratory experiment was conducted at a constant temperature of 30 °C. The microcosm experiment was conducted at elevated temperature in a similar manner as the laboratory experiment due to the following facts: (i) the temperature logger was placed at the bottom of the 70 cm deep basin while the flasks containing the cell culture floated on the surface and thus were half in contact with the air, so the interval of temperature fluctuation could be smaller, and (ii) the mean and median temperatures in the basin correspond

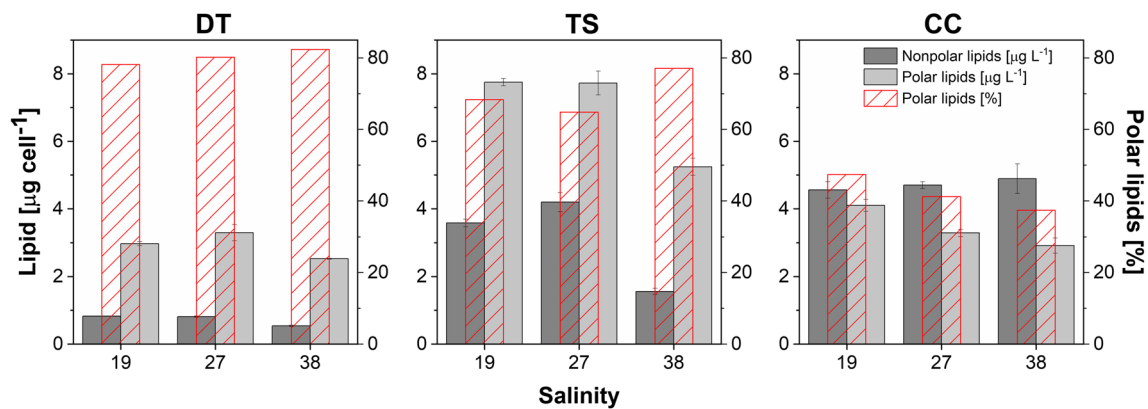


Fig. 8 Nonpolar and polar lipid content (solid columns) and the contribution of polar lipids to total cell lipids (pattern columns) of DT (*Dunaliella tertiolecta*), TS (*Tetraselmis suecica*), and CC (*Cylin-*

drotheca closterium) under environmental stressors in near-natural conditions. Data are shown as mean \pm SD

to 28.03 °C and 28.82 °C, respectively. The comparability of the two sets of experiments stems from the same objective, namely to study the response of microalgae to the effects of stressors, and the same experimental design, which included the setting of the same salinity levels and the corresponding temperature ranges, the collection of cell samples from all three species during the stationary growth phase, the equivalent replicability of the samples, the application of the identical protocols for sample characterization, the use of the same methods for cell characterization, and the measurement of the same set of variables.

Despite the limitations (no data on natural light intensity and inorganic carbon, as this was not part of our objective), cell growth of selected species was faster in the microcosm experiment than under laboratory conditions, indicating a complex and enhanced interaction of environmental stressors (light, temperature) that change throughout the day. This suggests that there is no inorganic carbon limitation. The response of microalgae (physiological activity, hydrophobicity) to environmental stressors showed a similar qualitative pattern to the response of cells to the salinity stressor under laboratory-controlled light intensity. This may suggest that salinity plays a primary role rather than diurnal variations in light and temperature, which could influence the quantitative magnitude of the corresponding variables and the discrepancy in the data.

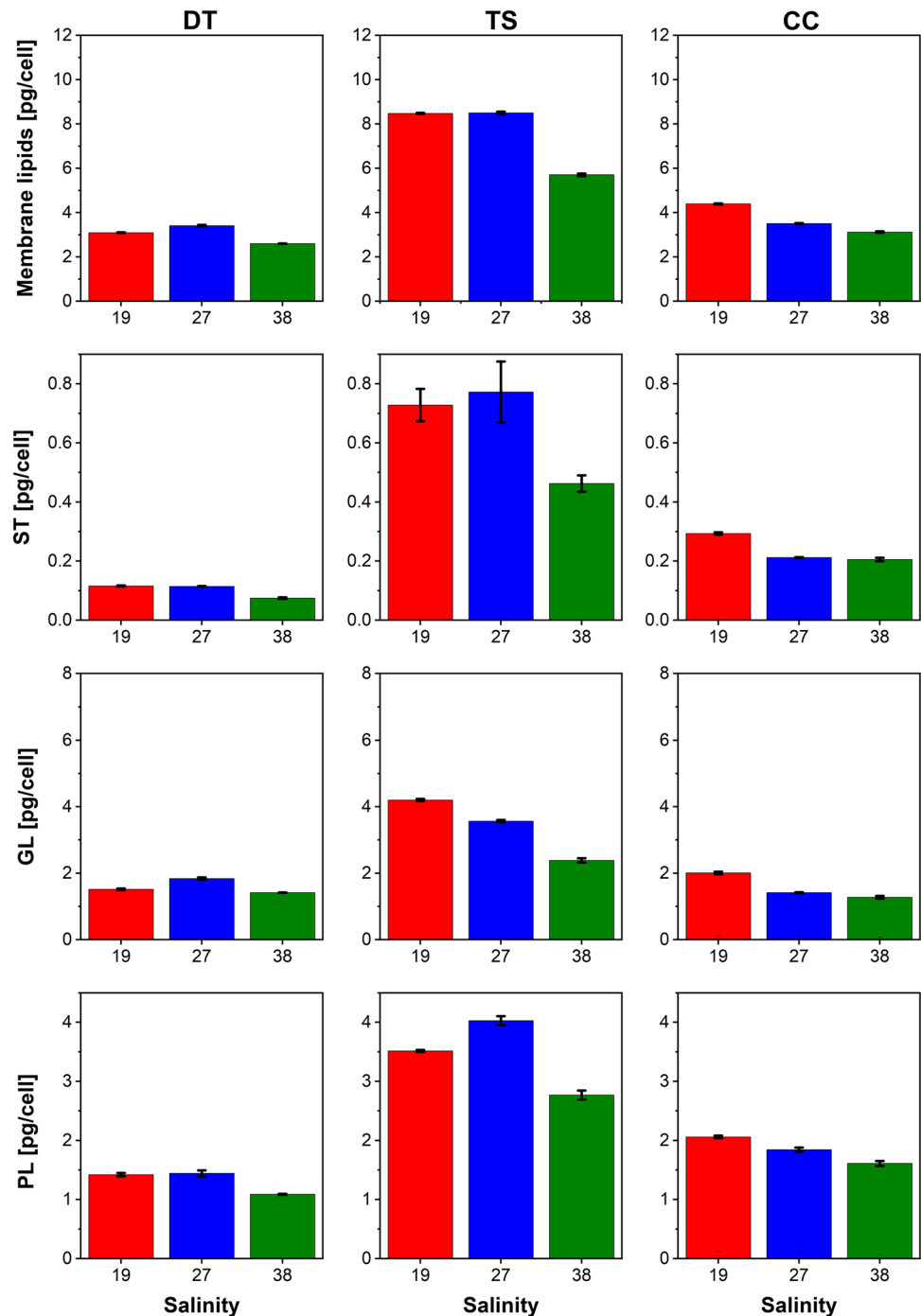
The first microalgal species, naked green DT, showed no change in cell speed and the cells vibrated on the spot under all selected environmental stressors in near-natural conditions (Fig. 4a, c). Interestingly, the mean cell speed of DT under environmental stressors was close to that under single stressor of salinity, indicating the thermotolerant nature of the cells (Ben-Amotz and Avron 1990; Jahnke and White 2003; Pick and Avidan 2017). When salinity was lowered to 19, responses such as decreased growth rate,

highest physiological activity, and increase in cell stiffness occurred. The increase in cell stiffness is most likely due to an increased concentration of sterols, which contribute to a decrease in membrane fluidity (Table S1, Figs. 5, 7, 9). These results are consistent with previous studies (Sheffer et al. 1986; Zelazny et al. 1995; Francavilla et al. 2010; Vrana et al. 2022). *Dunaliella* cells mainly maintained their hydrophilicity under environmental stressors (Figs. 8, S4), which was consistent with the predominant ratio of polar lipids (Fig. 9, Vrana et al. 2022).

In contrast to the laboratory study with DT cells using a single stressor (i.e., a salinity of 19 and a temperature of 18 °C were considered control conditions), the stiffness of the cells also increased, while DT showed hydrophobic behavior, as was also observed in an additional set of laboratory experiments and double stressors (salinity of 19 and a temperature of 30 °C, data not shown here). Thus, the response of microalgae appeared to be more pronounced when cells were stressed with salinity than with temperature under laboratory conditions (Novosel et al. 2022b).

For the second microalgal species, the green flagellate TS, the mean cell speed was about 3 times lower under near-natural conditions than under the same salinity and 18 °C in laboratory conditions. Although the cells of TS are surrounded by a calcite-encrusted theca, they were found to be sensitive to changes in salinity but tolerant of temperature. The predominant physiological activity was determined for the species TS at a salinity of 19 in both experiments, i.e., in the laboratory with defined light intensity and at constant temperature and in outdoor experiments where natural light and temperature varied throughout the day. This suggests that salinity can be considered as a primary stressor on physiological activity and cell stiffness of TS, while light and temperature variations could contribute to the variable magnitude and discrepancy in the data (Figs. 5 and 7).

Fig. 9 Membrane lipid content of DT (*Dunaliella tertiolecta*), TS (*Tetraselmis suecica*), and CC (*Cylindrotheca closterium*) under environmental stressors in near-natural conditions. Data are shown as mean \pm SD



Tetraselmis cells behaved in a balanced manner at salinities of 19 and 27 and elevated temperature (Table 1). A striking change occurred at a salinity of 38, at which the recorded cell growth rate was the highest (Table S1). TS showed hydrophobic behavior (Fig. S4), while the predominant content of polar lipids (Fig. 8) could also play an important role in sinking and cell adhesion to natural interfaces (Monteiro et al. 2023). Low hydrophobicity of TS cells was also observed when exposed to a single stressor under laboratory

conditions (salinity of 38, temperature of 18 °C, Novosel et al. 2022b) and at salinity of 38 and a temperature of 30 °C (data not shown here). The results also showed that cell stiffness decreased significantly under near-natural conditions in all species studied, in contrast to laboratory conditions, likely due to a complex interactions of environmental stressors under near-natural conditions.

The third species, the diatom CC covered with organosilicate, showed a different behavior than the flagellated

microalgae, i.e., with decreasing salinity the cells became softer, which could be related to the released organic matter changing the cell surface. In contrast, at salinity of 38, CC is stiffer and hydrophilic. The highest stiffness of CC could be related to minimal physiological activity (Table 1, Figs. 5, 7).

Regarding the nanomorphology of the cells, the results show that the size of DT cells (length and width) was largest at a salinity of 19 and an elevated temperature under near-natural conditions (Table S4), whereas the cells were largest at a salinity of 38 and a temperature of 18 °C under laboratory conditions (Novosel et al. 2022b). On the other hand, the cell size of TS was largest at a salinity of 38, both in microcosm at elevated temperature and in laboratory experiments at a temperature of 18 °C, demonstrating its temperature tolerance (Novosel et al. 2022a). Finally, the cell size of CC was constant in the microcosm experiment when exposed to environmental stressors, which could demonstrate the protective role of the cell wall. These results demonstrate a species- and stressor-specific response of the cells.

Regarding the nanostructural organization of the released organic matter, the predominance of globules and the absence of a fibrillar network structure were observed in the EPS of DT under near-natural conditions, as well as when the cells were exposed to salinity change under laboratory conditions (Novosel et al. 2022b). EPS from TS, grown under near-natural conditions at salinities of 9, 19, and 27, exhibited fibrillar network structures, whereas cells grown at salinity of 38 did not. The fibrillar network structure in the EPS of TS was also observed when the cells were exposed to altered salinity in the laboratory (Novosel et al. 2022b). The extracellular polymers of CC were mostly in globular form, whereas the fibrillar material was mostly present when the cells were exposed to a change in salinity under laboratory conditions (Novosel et al. 2022b).

At the molecular level, unfavorable growth conditions often lead to the accumulation of nonpolar lipids, mainly tryacylglycerols (Thompson 1996; Du and Benning 2016; Novak et al. 2019). Tryacylglycerols are stored in droplets in which they are surrounded by a phospholipid monolayer and proteins (Masclaux-Daubresse et al. 2020). The tryacylglycerol droplets are reused for the synthesis of polar lipids when conditions change (Thompson 1996). A study on the effects of temperature on tryacylglycerols and tryacylglycerol fatty acid composition of the microalga *Dunaliella viridis* found that increased temperature led to an accumulation of tryacylglycerols, while the fatty acid composition of tryacylglycerols was redistributed toward an increased proportion of saturated fatty acids (C16:0, C18:0, C20:0, C22:0, C24:0, and C26:0, Srirangan et al. 2015). Both cell content and the proportion of nonpolar lipids increased when two stressors (unfavorable temperature at ~ 30 °C and hypoosmotic shock

at salinities of 27 and 19) were combined in green algae DT and TS (Fig. 9). Since cell stiffness was also increased in these two microalgae (Fig. 7), we can assume that DT and TS produce tryacylglycerol droplets that contribute to cell stiffness. This is mainly because saturated fatty acids are more compactly bound than unsaturated ones (Niemelä et al. 2006) and thus contribute to cell stiffness. CC had the highest content of nonpolar lipids, indicating higher molecular changes under near-natural conditions (Fig. 8). Temperature as a stressor significantly increased sterol content in the membranes of all three algae studied (Fig. 9) compared to cultivation at 18 °C (Novosel et al. 2022b). However, while low salinity did not affect the sterol content of DT cells (Novosel et al. 2022b), the synergy of temperature and hypoosmotic stressors increased the ST content. The same trend was also observed in TS and CC. A similar pattern of increase in sterol content induced by an increase in water temperature in batch cultures of three dinoflagellates was also reported by Chen et al. (2019). The observed sterol increase was consistent with the fact that stability, fluidity, and permeability of the lipid bilayer depend on sterols (Benveniste 2004). Zelazny et al. (1995) also confirmed the role of plasma sterols in osmoregulation of two *Dunaliella* species. When *Dunaliella* cells were exposed to hyperosmotic shock, physiological activity increased in terms of inducing glycerol synthesis and synthesis of plasma membrane sterols (Zelazny et al. 1995). The exposure of *Tetraselmis striata* cells to various abiotic stresses such as nutrient deficiency, high light intensity, high salinity, and extreme temperatures, resulted in a decrease in biomass productivity, while lipid production was stimulated (Monteiro et al. 2023).

Glycolipid content of DT (Fig. 9) did not differ significantly under the influence of a single stressor (salinity, at 18 °C, Novosel et al. 2022b) or environmental stressors under near-natural conditions (~ 30 °C and for three salinities studied). The combination of the stressors, high temperature and hyposalinity, resulted in a significant increase in phospholipid content in DT cells (Fig. 9). Similar to DT, phospholipid content in TS and CC increased significantly at higher temperatures and when two stressors were combined (Fig. 9). The increase in phospholipid content could be due to increased saturated fatty acid content in phospholipids, as previously observed in the diatom *Chaetoceros pseudocurvisetus* (Vrana et al. 2023), where it facilitated membrane fluidization at high temperature. On the other hand, densely packed saturated fatty acids in the membranes indicate more phospholipids per unit membrane area (Gašparović et al. 2023, submitted), which in turn increases the content of phospholipids in cells. This suggests a greater role for phospholipids in thermal adaptation and adaptation in general. The presumed increase in phospholipid fatty acid saturation was reflected in the increased stiffness of DT at lower salinity and at a temperature of 30 °C (Fig. 8). While

hyposalinity stress alone leads to a decrease in glycolipid content in cells of TS and CC grown at 18 °C (Novosel et al. 2022b), the influence of environmental stressors leads to a substantial increase in the cellular content of glycolipids (Fig. 9), which are located in the photosynthetic apparatus (Siegenthaler 1998).

We conclude that the complex interplay of environmental stressors under near-natural conditions results in a species-specific response of microalgae that has not been integrated at the single cell level in this way. The three selected microalgae with different cell barrier complexity responded to environmental stressors, such as increased temperature and altered salinity, with behavioral, mechanical and molecular changes in near-natural environments. Under unfavorable conditions (salinity of 19), all microalgal species showed a low growth rate but maintained the highest physiological activity. The flagellated species, DT and TS, vibrated around the point and became stiffer, probably due to a higher content of sterols, while the hydrophilicity of the cells could be related to the high content of polar lipids. At the highest salinity, the growth rate of TS is highest and this species showed the most striking changes (e.g., loss of flagella) and exhibited the most pronounced hydrophobicity, which could favor the formation of aggregates, while the concentration of polar lipids could support cell adhesion to natural interfaces. Consequently, the response of TS could indicate progression to the cyst stage. In contrast, the hard, shell-covered diatom CC softened with decreasing salinity, accompanied by maximum physiological activity, which could lead to organic modification of the diatom surface.

Although the impacts of climate change on aquatic ecosystems are globally recognized (e.g., Velasco et al. 2019; Cooley et al. 2022), it is important to know how individual species at the base of the food chain respond to climate change-induced variability (Hernando et al. 2020; Van de Waal and Litchman 2020; Chien et al. 2023). These results provide new insights into the underlying mechanisms by which microalgae respond to environmental stress. They are important for predicting the effects of climate change on microbial community diversity, structure, and function (Malfatti et al. 2014; Cavicchioli et al. 2019) and for better understanding the ecological consequences of climate change on marine ecosystems.

Supplementary Information The online version contains supplementary material available at <https://doi.org/10.1007/s10811-023-03105-w>.

Acknowledgements We express our gratitude to Željko Šamec and Krešimir Rajaković from the Ruđer Bošković Institute for technical assistance in setting up the microcosm experiment. We acknowledge the networking under COST Action CA18238. We also thank the anonymous reviewer for valuable comments that helped improve this article.

Author contributions N.I.D.: conceptualization, methodology, visualization, supervision, project administration, funding acquisition,

writing-original draft; N.N.V., T.M.R., J.Z., M.L., I.D.Y., C.F.D., M.L.Z., I.V., and B.G.: investigation, methodology, formal analysis, visualization, writing-original draft; K.U.: methodology, formal analysis, visualization, statistical expertise, data interpretation, writing-original draft; L.H.: methodology, visualization; P.Ž.: visualization, writing-original draft; M.G.U.: conceptualization, writing-original draft, funding acquisition.

Funding This work was supported by the Croatian Science Foundation Project "From algal cell surface properties to stress markers for aquatic ecosystems" (IP-2018-01-5840), by the Croatian-French program "Cogito" partner Hubert Curien (Campus France n°46656ZC), by the Agence Nationale de la Recherche, JCJC project FLOTALG (ANR-18-CE43-0001-01).

Data availability The datasets generated during the current study are available from the corresponding authors on reasonable request.

Declarations

Competing interests The authors have no competing interests to declare that are relevant to the content of this article.

Conflict of interest We declare that we have no conflict of interest with any organizations or individuals that may have an effect on the results of our study. To the best of our knowledge, there are no financial, personal, or professional relationships that could be regarded as potential conflicts of interest.

Open Access This article is licensed under a Creative Commons Attribution 4.0 International License, which permits use, sharing, adaptation, distribution and reproduction in any medium or format, as long as you give appropriate credit to the original author(s) and the source, provide a link to the Creative Commons licence, and indicate if changes were made. The images or other third party material in this article are included in the article's Creative Commons licence, unless indicated otherwise in a credit line to the material. If material is not included in the article's Creative Commons licence and your intended use is not permitted by statutory regulation or exceeds the permitted use, you will need to obtain permission directly from the copyright holder. To view a copy of this licence, visit <http://creativecommons.org/licenses/by/4.0/>.

References

- Bautista-Chamizo E, Sendra M, Cid Á, Seoane M, Romano de Orte M, Riba I (2018) Will temperature and salinity changes exacerbate the effects of seawater acidification on the marine microalga *Phaeodactylum tricornutum*? *Sci Total Environ* 634:87–94
- Bauer DF (1972) Constructing confidence sets using rank statistics. *J Am Stat Assoc* 67:687–690
- Ben-Amotz A, Avron M (1990) The biotechnology of cultivating the halotolerant alga *Dunaliella*. *Trends Biotechnol* 8:121–126
- Benveniste P (2004) Biosynthesis and accumulation of sterols. *Annu Rev Plant Biol* 55:429–457
- Bligh EG, Dyer WJ (1959) A rapid method of total lipid extraction and purification. *Can J Biochem Physiol* 37:911–917
- Borowitzka MA (2018) The 'stress' concept in microalgal biology—homeostasis, acclimation and adaptation. *J Appl Phycol* 30:2815–2825
- Carter CM, Ross AH, Schiel DR, Howard-Williams C, Hayden B (2005) In situ microcosm experiments on the influence of nitrate

- and light on phytoplankton community composition. *J Exp Mar Biol Ecol* 326:1–13
- Cavicchioli R, Ripple WJ, Timmis KN, Azam F, Lars RB, Baylis M, Behrenfeld MJ, Boetius A, Boyd PW, Classen AT, Crowther TW, Danovaro R, Foreman CM, Huisman J, Hutchins DA, Jansson JK, Karl DM, Koskella B, Welch DBM, Martiny JBH, Moran MA, Orphan VJ, Reay DS, Remais JV, Rich VI, Singh BK, Stein LY, Stewart FJ, Sullivan MB, van Oppen MJ, Weaver HSC, Webb EA, Webster NS (2019) Scientists' warning to humanity: microorganisms and climate change. *Nat Rev Microbiol* 17:569–586
- Chien C-Te, Pahlow M, Schartau M, Li N, Oschlies A (2023) Effects of phytoplankton physiology on global ocean biogeochemistry and climate. *Sci Adv* 9:eadg1725
- Chen M, Bi R, Chen X, Ding Y, Zhang H, Li L, Zhao M (2019) Stoichiometric and sterol responses of dinoflagellates to changes in temperature, nutrient supply and growth phase. *Algal Res* 42:101609
- Cooley S, Schoeman D, Bopp L, Boyd P, Donner S, Ghebrehiwet DY, Ito S-I, Kiessling W, Martinetto P, Ojea E, Racault M-F, Rost B, Skern-Mauritzen M (2022) Ocean and coastal ecosystems and their services. In: Pörtner H-O, Roberts DC, Tignor M, Poloczanska ES, Mintenbeck K, Alegría A, Craig M, Langsdorf S, Löschke S, Möller V, Okem A, Rama B (eds) *Climate Change 2022: Impacts, Adaptation, and Vulnerability. Contribution of Working Group II to the Sixth Assessment Report of the Intergovernmental Panel on Climate Change*. Cambridge University Press, Cambridge, pp. 379–550
- Cronin G, Hay M (1996) Effects of light and nutrient availability on the growth, secondary chemistry, and resistance to herbivory of two brown seaweeds. *Oikos* 77:93–106
- Demir I, Lüchtfeld I, Lemen C, Dague E, Guiraud P, Zambelli T, Formosa Dague C (2021) Probing the interactions between air bubbles and (bio)interfaces at the nanoscale using FluidFM technology. *J Colloid Interface Sci* 604:785–797
- Demir-Yilmaz I, Novosel N, Levak Zorinc M, Mišić Radić T, Ftouhi MS, Guiraud P, Ivošević DeNardis N, Formosa-Dague C (2023a) Investigation of the role of cell hydrophobicity and EPS production in the aggregation of the marine diatom *Cylindrotheca closterium* under hypo-saline conditions. *Mar Environ Res* 188:106020
- Demir-Yilmaz I, Schiavone M, Esvan J, Guiraud P, Formosa-Dague C (2023b) Combining AFM, XPS and chemical hydrolysis to understand the complexity and dynamics of *C. vulgaris* cell wall composition and architecture. *Algal Res* 72:103102
- Domingues RB, Mosley BA, Nogueira P, Maia IB, Barbosa AB (2023) Duration, but not bottle volume, affects phytoplankton community structure and growth rates in microcosm experiments. *Water* 15:372
- Du ZY, Benning C (2016) Triacylglycerol accumulation in photosynthetic cells in plants and algae. In: Nakamura Y, Li-Beisson Y (eds) *Lipids in Plant and Algae Development*. Springer, Cham pp 172–205
- Farkas A, Pap B, Zsíros O, Patai R, Shetty P, Garab G, Bíró T, Ördög V, Maróti G (2023) Salinity stress provokes diverse physiological responses of eukaryotic unicellular microalgae. *Algal Res* 73:103155
- Flanjak L, Vrana I, Cvitešić Kušan A, Godrijan Novak T, Penezić A, Gašparović B (2022) The effects of high temperatures and nitrogen availability on the growth and composition of the marine diatom *Chaetoceros pseudocurvisetus*. *J Exp Bot* 73:4250–4265
- Gašparović B, Kazazić SP, Cvitešić A, Penezić A, Frka S (2015) Improved separation and analysis of glycolipids by Iatrosan thin-layer chromatography–flame ionization detection. *J Chromatogr A* 1409:259–267
- Gašparović B, Kazazić SP, Cvitešić A, Penezić A, Frka S (2017) Corrigendum to “Improved separation and analysis of glycolipids by Iatrosan thin-layer chromatography–flame ionization detection” [*J Chromatogr A* 1409 (2015) 259–267]. *J Chromatogr A* 1521:168–169
- Glibert PM, Cai W-J, Hall ER, Li M, Main KL, Rose KA, Testa JM, Vidyarathna NK (2022) Stressing over the complexities of multiple stressors in marine and estuarine systems. *Ocean-Land-Atmos Res* 2022:9787258
- Guillard RRL (1975) Culture of phytoplankton for feeding marine invertebrates. In: Smith WL, Chanley MH (eds) *Culture of Marine Invertebrate Animals: Proceedings—1st Conference on Culture of Marine Invertebrate Animals Greenport*. Springer, Boston, pp 29–60
- Häder D-P, Gao K (2015) Interactions of anthropogenic stress factors on marine phytoplankton. *Front Environ Sci* 3:14
- Hernando M, Varela D, Malanga G, Almandoz G, Schloss I (2020) Effects of climate-induced changes in temperature and salinity on phytoplankton physiology and stress responses in coastal Antarctica. *J Exp Mar Biol Ecol* 530–531:151400
- Hertz H (1881) Über die Berührung fester elastischer Körper. *J Reine Angew Math* 92:156–171
- Hollander M, Wolfe DA (1999) *Nonparametric Statistical Methods*. Wiley, New York
- Hunter KA, Liss PS (1981) Polarographic measurement of surface-active material in natural waters. *Water Res* 15:203–215
- Hutter JL, Bechhoefer J (1993) Calibration of atomic-force microscope tips. *Rev Sci Instrum* 64:1868–1873
- Ivošević DeNardis N, Pečar Ilić J, Ružić I, Novosel N, Mišić Radić T, Weber A, Kasum D, Pavlinska P, Katalin Balogh R, Hajdu B, Marček Chorvátová A, Gyurcsik B (2019) Algal cell response to laboratory-induced cadmium stress: a multimethod approach. *Eur Biophys J* 48:231–248
- Jahnke LS, White AL (2003) Long-term hyposaline and hypersaline stresses produce distinct antioxidant responses in the marine alga *Dunaliella tertiolecta*. *J Plant Physiol* 160:1193–1202
- Kholssi R, Lougraimzi H, Moreno-Garrido I (2023) Effects of global environmental change on microalgal photosynthesis, growth and their distribution. *Mar Environ Res* 184:105877
- Kim S-K (ed) (2015) *Handbook of marine microalgae*. Academic Press, London
- Malfatti F, Turk V, Tinta T, Mozetič P, Manganelli M, Samoa TJ, Ugalde JA, Kovač N, Stefanelli M, Antonioli M, Fonda-Umani S, Del Negro P, Cataletto B, Hozic A, Ivošević DeNardis N, Žutić V, Svetličić V, Mišić Radić T, Radić T, Fuks D, Azam F (2014) Microbial mechanisms coupling carbon and phosphorus cycles in phosphorus-limited northern Adriatic Sea. *Sci Tot Environ* 470–471:173–1183
- Masclaux-Daubresse C, d'Andrea S, Bouchez I, Cacas J-L (2020) Reserve lipids and plant autophagy. *J Exp Bot* 71:2854–2861
- Mišić Radić T, Čačković A, Penezić A, Dautović J, Lončar J, Omanović D, Juračić K, Ljubešić Z (2021) Physiological and morphological response of marine diatom *Cylindrotheca closterium* (Bacillariophyceae) exposed to cadmium. *Eur J Phycol* 56:24–36
- Mišić Radić T, Vukosav P, Komazec B, Formosa-Dague C, Domazet Jurašin D, Peharec Štefanić P, Čačković A, Juračić K, Ivošević DeNardis N (2022) Nanoplastic-induced nanostructural, nanomechanical, and antioxidant response of marine diatom *Cylindrotheca closterium*. *Water* 14:2163
- Monteiro I, Schüler LM, Santos E et al (2023) Two-stage lipid induction in the microalga *Tetraselmis striata* CTP4 upon exposure to different abiotic stresses. *Renew Energy* 208:693–701
- Murphy GEP, Romanuk TN, Worm B (2020) Cascading effects of climate change on plankton community structure. *Ecol Evol* 10:2170–2181
- Niemelä PS, Hyvönen MT, Vattulainen I (2006) Influence of chain length and unsaturation on sphingomyelin bilayers. *Biophys J* 90:851–863

- Novak T, Godrijan J, Marić Pfannkuchen D, Djakovac T, Medić N, Ivančić I, Mlakar M, Gašparović B (2019) Global warming and oligotrophication lead to increased lipid production in marine phytoplankton. *Sci Total Environ* 668:171–183
- Novosel N, Kasum D, Žutinić P, Legović T, Ivošević DeNardis N (2020) Short-term effect of cadmium on the motility of three flagellated algal species. *J Appl Phycol* 32:4057–4067
- Novosel N, Mišić Radić T, Zemla J, Lekka M, Čačković A, Kasum D, Legović T, Žutinić P, Gligora Udovič M, Ivošević DeNardis N (2022a) Temperature-induced response in algal cell surface properties and behaviour: an experimental approach. *J Appl Phycol* 34:243–259
- Novosel N, Mišić Radić T, Levak Zorinc M, Zemla J, Lekka M, Vrana I, Gašparović B, Horvat L, Kasum D, Legović T, Žutinić P, Gligora Udovič M, Ivošević DeNardis N (2022b) Salinity induced chemical, mechanical and behavioral changes in marine microalgae. *J Appl Phycol* 34:1293–1309
- Pick U, Avidan O (2017) Triacylglycerol is produced from starch and polar lipids in the green alga *Dunaliella tertiolecta*. *J Exp Bot* 68:4939–4950
- Pillet F, Dague E, Pečar Ilić J, Ružić I, Rols M-P, Ivošević DeNardis N (2019) Changes in nanomechanical properties and adhesion dynamics of algal cells during their growth. *Bioelectrochemistry* 128:154–162
- Pletikapić G, Berquand A, Mišić Radić T, Svetličić V (2012) Quantitative nanomechanical mapping of marine diatom in seawater using peak force tapping atomic force microscopy. *J Phycol* 48:174–185
- Pletikapić G, Ivošević DeNardis N (2017) Application of surface analytical methods for hazardous situation in the Adriatic Sea: Monitoring of organic matter dynamics and oil pollution. *Nat Hazards Earth Syst Sci* 17:31–44
- RStudio Team (2023) RStudio: Integrated Development Environment for R. Posit Software, PBC, Boston, MA
- R Core Team (2022) R: A language and environment for statistical computing. R Foundation for Statistical Computing, Vienna, Austria. <https://www.R-project.org/>
- Royston P (1995) Remark AS R94: A remark on Algorithm AS 181: The WW test for normality. *Appl Stat* 44:551
- Sader JE, Larson I, Mulvaney P, White LR (1995) Method for the calibration of atomic force microscope cantilevers. *Rev Sci Instrum* 66:3789–3798
- Schriber CL, Venable ME (2019) The Effects of Environmental Stressors on Aggregation in *Parachlorella kessleri*. *J Environ Protect* 10:1657–1676
- Siegenthaler P-A (1998) Molecular organization of acyl lipids in photosynthetic membranes of higher plants. In: Siegenthaler PA, Murata N (eds) *Lipids in photosynthesis*. Kluwer, Dordrecht, pp 119–144
- Sneddon IN (1965) The relation between load and penetration in the axisymmetric boussinesq problem for a punch of arbitrary profile. *Int J Eng Sci* 3:47–57
- Srirangan S, Sauer ML, Howard B, Dvora M, Dums J, Backman P, Sederoff H (2015) Interaction of temperature and photoperiod increases growth and oil content in the marine microalgae *Dunaliella viridis*. *PLoS One* 10:e0127562
- Svetličić V, Balnois E, Žutić V, Chevalet J, Hozić Zimmermann A, Kovač S, Vdović N (2006) Electrochemical detection of gel microparticles in seawater. *Croat Chem Acta* 79:107–113
- Thompson GA (1996) Lipids and membrane function in green algae. *Biochim Biophys Acta - Lipids Lipid Metab* 1302:17–45
- Van de Waal DB, Litchman E (2020) Multiple global change stressor effects on phytoplankton nutrient acquisition in a future ocean. *Phil Trans R Soc Lond B* 375:20190706
- Velasco J, Gutiérrez-Cánovas C, Botella-Cruz M, Sánchez-Fernández D, Arribas P, Carbonell JA, Millán A, Pallarés S (2019) Effects of salinity changes on aquatic organisms in a multiple stressor context. *Philos Trans R Soc Lond B* 374:20180011
- Vrana I, Alempijević SB, Novosel N, Ivošević DeNardis N, Zigon D, Ogrinc N, Gašparović B (2022) Hyposalinity induces significant polar lipid remodeling in the marine microalga *Dunaliella tertiolecta* (Chlorophyceae). *J Appl Phycol* 34:1457–1270
- Vrana I, Gašparović B, Geček S, Godrijan J, Novak T, Kazazić SP, Mlakar M, Kužat N, Pfannkuchen M, Marić Pfannkuchen D (2023) Successful acclimation of marine diatoms *Chaetoceros curvisetus/pseudocurvisetus* to climate change. *Limnol Oceanogr* 63:S158–S173
- Wu X, Liu H, Ru Z, Tu G, Xing L, Ding Y (2021) Meta-analysis of the response of marine phytoplankton to nutrient addition and seawater warming. *Mar Environ Res* 168:105294
- Zelazny AM, Shaish A, Pick U (1995) Plasma-membrane sterols are essential for sensing osmotic changes in the halotolerant alga *Dunaliella*. *Plant Physiol* 109:1395–1403
- Zhang X, Tan L, Cai Q, Ye L (2022) Environmental factors indirectly reduce phytoplankton community stability via functional diversity. *Front Ecol Evol* 10:990835
- Žutić V, Svetličić V, Ivošević N, Hozić A, Pečar O (2004) Northern Adriatic mesocosm experiment Rovinj 2003: dynamics of organic microparticles studied by the electrochemical technique. *Period Biol* 106:67–74

Publisher's Note Springer Nature remains neutral with regard to jurisdictional claims in published maps and institutional affiliations.